BACHELOR'S DEGREE THESIS

Degree in Mathematics

Title: Analysis of periodic solutions of the system Janus-Epimetheus

Author: Luis Huesca Molina

Advisor: Jaume Soler Villanueva

Department: Departament d'Enginyeria Civil i Ambiental

Academic year: 2015/2016

UNIVERSITAT POLITÈCNICA DE CATALUNYA
BARCELONATECH
Facultat de Matemàtiques i Estadística

Universitat Politècnica de Catalunya
Facultat de Matemàtiques i Estadística

Bachelor's Degree Thesis

Analysis of periodic solutions of the system Janus-Epimetheus

Luis Huesca Molina

Directors:
Jaume Soler Villanueva
Mercè Ollè Torner

Abstract

In this project we develop a 2-dimensional model for the motion of the coorbital moons of Saturn, Janus and Epimetheus. In order to make it close to the real system the model includes the gravitational field due to the oblateness of Saturn and slightly elliptic orbits for the satellites. Numerical explorations show the existence of families of periodic orbits whose elements are close to the real ones and suggest a rich and complex structure of periodic or almost-periodic motions in the phase space.

The equations of motion are numerically integrated with a (7,8)-order embedded Runge-Kutta-Fehlberg routine called from MATLAB's *fsolve* native function.

Keywords

Numerical methods, coorbital satellites, dynamical systems, periodic solutions

Contents

1 Introduction

In 1980 two satellites of Saturn, now named Janus and Epimetheus, were imaged for the first time by the *Voyager 1* spacecraft. At that time, Janus had a semi-major axis $a_J = 151472$ km, while Epimetheus had $a_E = 151422$ km. Thus, their orbital separation was of 50 km. Although they were not spherical, they had approximate mean diameters of $r_J = 175$ km and $r_E = 105$ km. At the moment of the image, they were approximately 180º apart, and because of their distances and sizes, a quick analysis suggested a collision some time in the near future.

In the end, there was no collision. It was seen that the orbits are performing a horseshoe orbit, that is, in a rotating frame with Saturn fixed in the origin and one of the satellites fixed on the horizontal axis, the other satellite describes an orbit that looks like a horseshoe.

The masses of the satellites are not negligible and when they approach each other the mutual perturbation results in the satellites swapping their orbits.

The aim of this work is to develop a model that fits the real phenomen to analyse the existence of periodic or almost-periodic solutions. In [6] some results are obtained with a circular model, but the orbits of both satellites are perturbations of elliptic orbits, and because of that we are interested in developing an elliptic model.

We said that the orbital separation between both orbits was around 50 km, and according to data from JPL (Jet Propulsion Laboratory), the orbits are slightly elliptic so the distances of each satellite to Saturn can vary some 1500 km, which is a large number compared to the difference of 50 km given above. In our model we also want to add the oblateness of Saturn, as it makes some changes in the gravitational field. For circular orbits it is almost unnoticeable, but for elliptic orbits, it has some effects on the orbital elements which cannot be neglected.

Although the more realistic model involves both masses being different from zero, an approximation can be done taking one of them as zero, which is called the restricted problem, which makes some things easier. The differences between both models are explained.

Finding periodic solutions with these equations is harder than in the circular model, because having elliptic orbits adds some problems. For example, in the rotating frame, circular periodic orbits are easily seen but elliptic orbits cannot be easily spotted.

Because of this, some properties and symmetries of the equations are proved and then, some numerical explorations are carried out to find solutions that satisfy these symmetries to then assure that the problem has families of periodic or almost-periodic solutions.

High accuracy algorithms are important for this problem, as it is very sensitive and low accuracy could end in false results. Because of that, high order differential equations solvers are developed and other high order algorithms too.

Our interest in giving some first explorations on periodic solutions is to clear the way to find these solutions sistematically or by other analytical methods.

This thesis is organized as follows:

1. In Section 2, equations for the n-body problem are seen.
2. In Section 3 the oblateness of a central body is modelled and added to the equations.
3. Lemmas and symmetries of the equations are studied in Section 4.
4. In Section 5, simulations are carried out to use what is done in previous sections.
5. Section 6 ends with some conclusions and proposals for future work.

2 Three body problem: Saturn, Janus and Epimetheus

2.1 Mathematical Model: The n-body problem

We start by deducing a simple model to describe the problem using Newton's universal gravitation law.

Given a point mass M with coordinates $\mathbf{x}_0$, the gravitational potential generated by the mass is

$$V(\mathbf{x}) = -\frac{GM}{\|\mathbf{x} - \mathbf{x}_0\|}$$

where G is the universal gravitational constant.

The gravitational field created is the vector field

$$\mathbf{F}(\mathbf{x}) = -\nabla V(\mathbf{x}) = -\frac{GM}{\|\mathbf{x} - \mathbf{x}_0\|^2} \frac{\mathbf{x} - \mathbf{x}_0}{\|\mathbf{x} - \mathbf{x}_0\|}$$

By Newton's laws, the motion equations of a point mass in this vector field is given by

$$\ddot{\mathbf{x}} = \mathbf{F}(\mathbf{x})$$

In $\mathbb{R}^3$, if we have n point masses, then each mass is affected by the gravitational field of each other of the $n-1$ masses. If any of the masses m_i is zero, that is, the mass is so small that it does not influence the other masses but it is influenced by them, the problem is called a restricted problem.

The equations of motion are

$$m_i \ddot{\mathbf{x}}_i = \sum_{j=1, j\neq i}^{n} -\frac{G m_i m_j}{\|\mathbf{x}_i - \mathbf{x}_j\|^2} \frac{\mathbf{x}_i - \mathbf{x}_j}{\|\mathbf{x}_i - \mathbf{x}_j\|} \qquad i = 1, ..., n$$

The centre of masses, given by

$$\mathbf{x}_{CM} = \frac{\sum_{i=1}^n m_i \mathbf{x}_i}{\sum_{i=1}^n m_i}$$

moves with constant velocity, because

$$\begin{aligned}
\ddot{\mathbf{x}}_{CM} &= \frac{1}{M} \sum_{i=1}^{n} m_i \ddot{\mathbf{x}}_i \\
&= \frac{1}{M} \sum_{i=1}^{n} m_i \sum_{j=1, j\neq i}^{n} -\frac{G m_i m_j}{\|\mathbf{x}_i - \mathbf{x}_j\|^2} \frac{\mathbf{x}_i - \mathbf{x}_j}{\|\mathbf{x}_i - \mathbf{x}_j\|} \\
&= \frac{1}{M} \sum_{\substack{i,j \\ i\neq j}}^{n} -\frac{G m_i m_j}{\|\mathbf{x}_i - \mathbf{x}_j\|^2} \frac{(\mathbf{x}_i - \mathbf{x}_j) + (\mathbf{x}_j - \mathbf{x}_i)}{\|\mathbf{x}_i - \mathbf{x}_j\|} \\
&= 0
\end{aligned}$$

where $M = \sum_{i=1}^n m_i$.

Because of this result, we can take the origin of coordinates on the centre of mass.

With this coordinates we can omit one of the bodies equations, as it can be obtained from the other $n-1$ bodies positions and the centre of mass (the origin of coordinates).

There are still four first integrals left (i.e. functions which are constant along the trajectories): the energy of the system and the three components of the angular momentum.

If $n = 2$, we have the two-body problem. This problem is equivalent to the motion of one body under an inverse-square law with origin at the centre of mass of the system. The other body moves so that the centre of mass remains fixed at the origin.

If we consider two bodies of masses m_1 and m_2, and positions $\mathbf{r}_1$ and $\mathbf{r}_2$, their relative position vector is $\mathbf{r} = \mathbf{r}_1 - \mathbf{r}_2$. The forces on each body are

$$\mathbf{F}_{12} = -G\frac{m_1 m_2}{r^2}\frac{\mathbf{r}}{r}$$

$$\mathbf{F}_{21} = -G\frac{m_1 m_2}{r^2}\frac{-\mathbf{r}}{r} = -\mathbf{F}_{12}$$

Using Newton's second law on each body,

$$m_1\ddot{\mathbf{r}}_1 = \mathbf{F}_{12}$$

$$m_2\ddot{\mathbf{r}}_2 = \mathbf{F}_{21}$$

Dividing the equation of each body by its mass and substracting them, we get

$$\ddot{\mathbf{r}}_1 - \ddot{\mathbf{r}}_2 = \frac{\mathbf{F}_{12}}{m_1} - \frac{\mathbf{F}_{21}}{m_2} = \mathbf{F}_{12}\left(\frac{1}{m_1} + \frac{1}{m_2}\right)$$

So we finally get

$$\ddot{\mathbf{r}} = \mathbf{F}_{12}\left(\frac{1}{m_1} + \frac{1}{m_2}\right)$$

If we consider the mass $\mu = \frac{m_1 m_2}{m_1 + m_2}$, the equation for $\mathbf{r}$ is

$$\mu\ddot{\mathbf{r}} = \mathbf{F}_{12}$$

This is the problem of a central force for one mass, which is called the Kepler problem.

It is well-known that the solution can be expressed in terms of a keplerian orbit with six orbital elements.

2.2 Orbital elements of Kepler motion

The Kepler problem is the motion of a particle of mass m under a central force of modulus inverse square proportional. The equation is

$$\mu\ddot{\mathbf{x}} = \mathbf{F}$$

where $\mathbf{F} = \frac{K}{\|\mathbf{x}\|^2}\frac{\mathbf{x}}{\|\mathbf{x}\|}$. In this case, the first integrals of the energy and the angular momentum are given by

$$E(\mathbf{x}, \dot{\mathbf{x}}) = \frac{1}{2}m\dot{\mathbf{x}}^2 - \frac{Gm}{\|\mathbf{x}\|}$$

$$\mathbf{M}(\mathbf{x}, \dot{\mathbf{x}}) = \mathbf{x} \times m\dot{\mathbf{x}}$$

If the angular momentum is not zero, the motion of the particle remains on the plane perpendicular to the angular momentum vector, usually known as the invariant plane.

Depending on the value E of the energy, the orbits can be of different types:

- Eliptic if $E < 0$
- Parabolic if $E = 0$
- Hiperbolic if $E > 0$

We are interested in the first case. The parameters and position of the ellipse are usually called the *orbital elements* as shown in Figure 1.

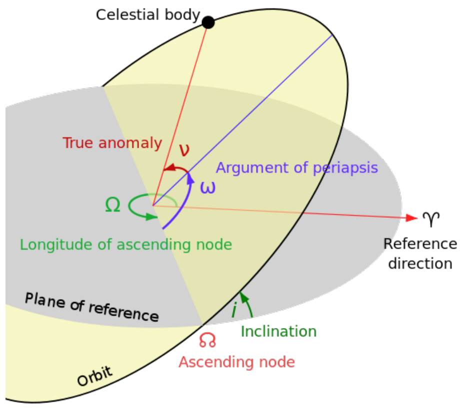

Figure 1: Orbital Elements

- e: eccentricity $= \frac{r_a - r_p}{r_a + r_p}$ where r_p and r_a are the periapsis and apoapsis distances
- a: semi-major axis $= \frac{1}{2|E|}$
- i: inclination of the orbital plane
- Ω: longitude of the ascending node
- ω: argument of periapsis
- ν: true anomaly

It is well-known (see [3]) that the ellipse is given in polar coordinates (r, θ) by

$$r(\theta) = \frac{a(1-e^2)}{1 + e\cos(\theta - \omega)}$$

The apoapsis is the furthest point of the gravitational center. We can calculate its distance by $r_a = a(1+e)$. On the other hand, the periapsis is the closest point and its distance can be calculated by $r_a = a(1-e)$. The apsis line is the line that joins both the periapsis and apoapsis. Its length is $2a$ and it passes through the apoapsis, the periapsis and the gravitational centre.

In the reference plane, given three different points of an orbit we can determine its elements with the following procedure. As explained in [3], let's call these points P_1, P_2 i P_3 and let's suppose they are given in polar coordinates $P_i = (r_i, \theta_i)$, $i = 1, 2, 3$.

If we call $P = e\cos(\omega)$, $Q = e\sin(\omega)$ and $p = a(1-e^2)$, we have the following system of equations:

$$\begin{cases} \frac{p}{r_1} - P\cos(\theta_1) - Q\sin(\theta_1) = 1 \\ \frac{p}{r_2} - P\cos(\theta_2) - Q\sin(\theta_2) = 1 \\ \frac{p}{r_3} - P\cos(\theta_3) - Q\sin(\theta_3) = 1 \end{cases}$$

Solutions for p, P, Q are given by:

$$p = \frac{r_1 r_2 r_3[\sin(\theta_3 - \theta_2) + \sin(\theta_1 - \theta_3) + \sin(\theta_2 - \theta_1)]}{r_2 r_3 \sin(\theta_3 - \theta_2) + r_1 r_3 \sin(\theta_1 - \theta_3) + r_1 r_2 \sin(\theta_2 - \theta_1)}$$

$$P = \frac{r_1(r_2 - r_3)\sin\theta_1 + r_2(r_3 - r_1)\sin\theta_2 + r_3(r_1 - r_2)\sin\theta_3}{r_2 r_3 \sin(\theta_3 - \theta_2) + r_1 r_3 \sin(\theta_1 - \theta_3) + r_1 r_2 \sin(\theta_2 - \theta_1)}$$

$$Q = \frac{r_1(r_3 - r_2)\cos\theta_1 + r_2(r_1 - r_3)\cos\theta_2 + r_3(r_2 - r_1)\cos\theta_3}{r_2 r_3 \sin(\theta_3 - \theta_2) + r_1 r_3 \sin(\theta_1 - \theta_3) + r_1 r_2 \sin(\theta_2 - \theta_1)}$$

Here we can isolate the orbital elements:

$$e = \sqrt{P^2 + Q^2}$$

$$\omega = \tan^{-1}\left(\frac{Q}{P}\right)$$

$$a = \frac{p}{1 - e^2}$$

2.3 Perturbed Kepler motion

Now let's introduce what is a perturbed Kepler problem. Given

$$\dot{\mathbf{x}} = \mathbf{f}(\mathbf{x})$$

a Kepler problem, if we add a perturbation

$$\dot{\mathbf{x}} = \mathbf{f}(\mathbf{x}) + \mathcal{E}\mathbf{g}(\mathbf{x})$$

with $\mathcal{E} > 0$ small, the solutions may behave a bit differently. In particular, the orbital elements may not be constant. This is specially useful when talking about the three-body problem or adding oblateness to the potential function of the bodies.

A solution of a perturbed problem can usually be approximated by a keplerian orbit with the appropriate elements. For example, let's consider the two central forces problem for a mass, one on the origin of coordinates $(x_1, y_1) = (0, 0)$ and the other one in $(x_2, y_2) = (0, -1)$. If the attraction made by the second one is much smaller compared to the attraction made by the first one, ie $\mathcal{E}$ is very small, then a solution can be seen in Figure 2, given by the initial conditions $(x_0, y_0) = (1, 0)$ and $(\dot{x}_0, \dot{y}_0) = (0, 0.9)$.

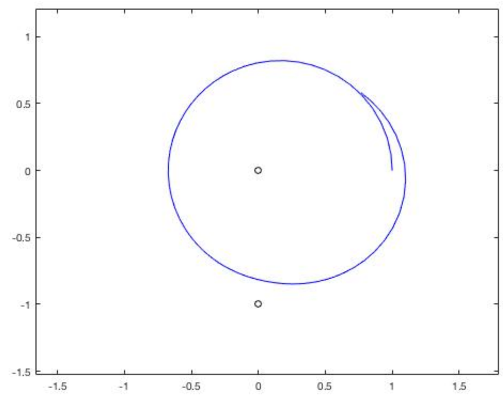

Figure 2: Perturbed orbit numerically computed

Using the formulae described before for the orbital elements, we can find a perfect ellipse that approximates well this solution. In particular, a Keplerian orbit with elements $a = 0.8562$,$e = 0.2206$,-3.1583 can be seen as a very good approximation of the real solution.

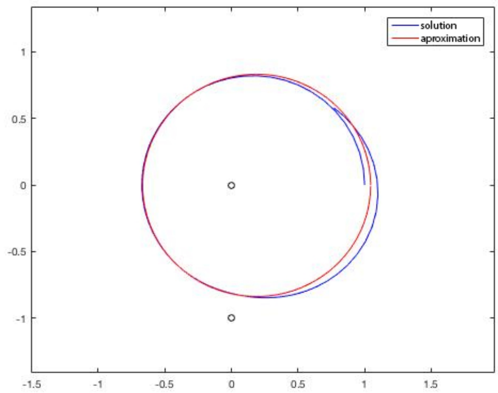

Figure 3: Perturbed orbit numerically computed with ellipse calculated from three points

Finally, we end with a definition of osculating orbit: given a perturbed Kepler problem, with solution $(x(t), y(t), \dot{x}(t), \dot{y}(t))$, for each point at time $t = T$, the osculating orbit of that point is the unique solution of the non-perturbed Kepler problem with initial conditions $(x(T), y(T), \dot{x}(T), \dot{y}(T))$.

2.4 Nondimensionalization

In our reference frame, Saturn will be on the origin of coordinates. This will not pose any problem as the centre of mass is almost on Saturn's centre, as its mass is much higher than the masses of both satellites. For simplicity, we will work in the plane but this does not change our results too much.
Let $\mathbf{x}_E$ and $\mathbf{x}_J$ be the position vectors of each body, using the general formula described before, our system of differential equations reads as follows:

$$\begin{cases} M_E \ddot{\mathbf{x}}_E = -G\frac{M_S M_E}{\|\mathbf{x}_E\|^2}\frac{\mathbf{x}_E}{\|\mathbf{x}_E\|} - G\frac{M_E M_J}{\|\mathbf{x}_E-\mathbf{x}_J\|^2}\frac{\mathbf{x}_E-\mathbf{x}_J}{\|\mathbf{x}_E-\mathbf{x}_J\|} \\ M_J \ddot{\mathbf{x}}_J = -G\frac{M_S M_J}{\|\mathbf{x}_J\|^2}\frac{\mathbf{x}_J}{\|\mathbf{x}_J\|} - G\frac{M_J M_E}{\|\mathbf{x}_J-\mathbf{x}_E\|^2}\frac{\mathbf{x}_J-\mathbf{x}_E}{\|\mathbf{x}_J-\mathbf{x}_E\|} \end{cases}$$

As we are working in the plane our system has 2 bodies $\times$ 2 coordinates $\times$ 2 equations $=$ 8 equations. In a Hamiltonian formalism of the problem, we have 4 degrees of freedom.

It is important to talk about each constant and what does it mean:

- G: universal gravitational constant, its value is $G = 6.673 \times 10^{-11}$ and its units are $\frac{N\cdot m^2}{\text{kg}^2}$
- M_S: Saturn's mass, its value is $M_S = 5.683 \times 10^{26}$ kg
- M_E: Epimetheus mass, with $m_E = 5.266 \times 10^{17}$ kg
- M_J: Janus mass, with $m_J = 1.8975 \times 10^{18}$ kg

To make equations more simple and easier to work with, we will rescale them and we will obtain a new system. To do it we will use the constants we saw before and their units.
Fundamental magnitudes are measured with:

$$\text{mass} = [\text{kg}] \quad \text{length} = [\text{m}] \quad \text{time} = [s]$$

The average orbital radius of Epimetheus and Janus are:

$$r_E = 151472 \times 10^3 \text{ m} \quad r_J = 151422 \times 10^3 \text{ m}$$

With these numbers, and the ones seen before, we define a new scale:

$$x^* = \frac{1}{r_E} x$$

$$t^* = \sqrt{\frac{GM_S}{r_E^3}} t$$

To simplify notation, we will omit the asterisks on the names of the variables. The rescaled equations are:

$$\begin{cases} \ddot{\mathbf{x}}_E = -\frac{1}{\|\mathbf{x}_E\|^2}\frac{\mathbf{x}_E}{\|\mathbf{x}_E\|} - \frac{m_J}{\|\mathbf{x}_E-\mathbf{x}_J\|^2}\frac{\mathbf{x}_E-\mathbf{x}_J}{\|\mathbf{x}_E-\mathbf{x}_J\|} \\ \ddot{\mathbf{x}}_J = -\frac{1}{\|\mathbf{x}_J\|^2}\frac{\mathbf{x}_J}{\|\mathbf{x}_J\|} - \frac{m_E}{\|\mathbf{x}_J-\mathbf{x}_E\|^2}\frac{\mathbf{x}_J-\mathbf{x}_E}{\|\mathbf{x}_J-\mathbf{x}_E\|} \end{cases}$$

where $m_E = \frac{M_E}{M_S}$ and $M_J = \frac{M_J}{M_S}$.
Transforming the system into a first order system for each body, finally, the system results in the following:

$$\begin{cases} \dot{\mathbf{x}}_E = \mathbf{v}_E \\ \dot{\mathbf{x}}_J = \mathbf{v}_J \\ \dot{\mathbf{v}}_E = -\frac{1}{\|\mathbf{x}_E\|^2}\frac{\mathbf{x}_E}{\|\mathbf{x}_E\|} - \frac{m_J}{\|\mathbf{x}_E-\mathbf{x}_J\|^2}\frac{\mathbf{x}_E-\mathbf{x}_J}{\|\mathbf{x}_E-\mathbf{x}_J\|} \\ \dot{\mathbf{v}}_J = -\frac{1}{\|\mathbf{x}_J\|^2}\frac{\mathbf{x}_J}{\|\mathbf{x}_J\|} - \frac{m_E}{\|\mathbf{x}_J-\mathbf{x}_E\|^2}\frac{\mathbf{x}_J-\mathbf{x}_E}{\|\mathbf{x}_J-\mathbf{x}_E\|} \end{cases}$$

In this scale, another important value to take into account is the average distance between both orbits, which is 50000 m. In our new scale this distance is

$$\epsilon = \frac{50000}{r_E} = 0.33 \times 10^{-3}$$

3 Saturn's oblateness

3.1 Modelling the oblateness

The equations we have seen until now are true if each body is considered as a point mass, but it is obvious that a celestial body is not a point mass. Celestial bodies occupy a certain volume, and their mass is distributed in this volume.

Because of that, to calculate the real force between two bodies we can use the force between two point masses and integrate for the volumes of both bodies. That is:

$$\mathbf{F} = -G \int_{V_1} \int_{V_2} \frac{\rho_1(\mathbf{x}_1)\rho_2(\mathbf{x}_2)}{\|\mathbf{x}_2 - \mathbf{x}_1\|^2} \frac{\mathbf{x}_2 - \mathbf{x}_1}{\|\mathbf{x}_2 - \mathbf{x}_1\|} d\mathbf{x}_2 d\mathbf{x}_1$$

where ρ_1 and ρ_2 are the densities of the bodies, and V_1 and V_2 are their volumes. It is obvious that this integral won't be the same as the point masses case.

Although we cannot calculate this integral explicitely, we can give an approximation by Legendre expansions. As it can be seen in [1], the potential generated by a massive body symmetric with respect to the z-axis, responding only to rotational forces is given in spherical coordinates (r, θ, ϕ) by

$$V = -\frac{GM_S}{r} \left[1 - \sum_{n=1}^{\infty} \left(\frac{R_S}{r} \right)^{2n} J_{2n} P_{2n}(\sin\phi) \right]$$

where ϕ is the colatitude (angle on a plane which contains the z-axis measured from the semiaxis of positive z), the coefficients J_{2n} are determined by geometric characteristics of the body and P_{2n} are Legendre polynomials. Notice that if we take out the sum, we would have the potential for the point mass that we already saw.

We will consider the first order approximation, that is, the expansion up to the first term of the sum. Our potential then is

$$V = -\frac{GM_S}{r} + \frac{GM_S R_S^2 J_2}{r^3} \frac{1}{2} \left(3\sin^2\phi - 1 \right)$$

The term $(3\sin^2(\phi) - 1)$ is only important in three dimensions, and because of that we can just ommit it to make things easier (considering $\sin^2\phi = 0$ so that it is equal to -1).

Finally, as we did with the previous potential, the gravitational field created by this potential is:

$$F = -\nabla V = -\frac{GM_S}{r^2} \frac{\mathbf{r}}{r} - \frac{3}{2} \frac{GM_S R_S^2 J_2}{r^4} \frac{\mathbf{r}}{r}$$

3.2 Model for Saturn and the coorbitals

Using the same scale that we used in section 2.3, we obtain the following force:

$$F^* = -\frac{1}{{r^*}^2} \frac{\mathbf{r}^*}{r^*} - \frac{3}{2} \frac{{R_S^*}^2 J_2}{{r^*}^4} \frac{\mathbf{r}^*}{r^*}$$

where $R_S^* = \frac{R_S}{r_E} = \frac{58232}{151472} = 0.384$. Notice that the value J_2 is the same, as it is a nondimensional magnitude and in the case of Saturn it is $J_2 = 0.0163$.

Finally, the system with oblateness, once nondimensionalized, results to be the following:

$$\begin{cases} \dot{\mathbf{x}}_E = \mathbf{v}_E \\ \dot{\mathbf{x}}_J = \mathbf{v}_J \\ \dot{\mathbf{v}}_E = -\frac{1}{\|\mathbf{x}_E\|^2} \frac{\mathbf{x}_E}{\|\mathbf{x}_E\|} - \frac{m_J}{\|\mathbf{x}_E - \mathbf{x}_J\|^2} \frac{\mathbf{x}_E - \mathbf{x}_J}{\|\mathbf{x}_E - \mathbf{x}_J\|} - \frac{3}{2} \frac{{R_S^*}^2 J_2}{\|\mathbf{x}_E\|^4} \frac{\mathbf{x}_E}{\|\mathbf{x}_E\|} \\ \dot{\mathbf{v}}_J = -\frac{1}{\|\mathbf{x}_J\|^2} \frac{\mathbf{x}_J}{\|\mathbf{x}_J\|} - \frac{m_E}{\|\mathbf{x}_J - \mathbf{x}_E\|^2} \frac{\mathbf{x}_J - \mathbf{x}_E}{\|\mathbf{x}_J - \mathbf{x}_E\|} - \frac{3}{2} \frac{{R_S^*}^2 J_2}{\|\mathbf{x}_J\|^4} \frac{\mathbf{x}_J}{\|\mathbf{x}_J\|} \end{cases}$$

This is the system that we will use. With this system, we will do simulations with two different models:

- Restricted problem: $m_E = 0$, which makes the second body independent of the motion of the first one.
- Full problem: $m_E \neq 0$ and $m_J \neq 0$

3.3 Effects on keplerian motion

As we have seen, oblateness gives us different equations. Because of that,the solutions show different behaviour.
If we recall the orbital elements described on section 2.4., with oblateness, these elements do not remain constant. Actually, the element that changes the most is the argument of the periapsis, as explained in [7]. More concretely, $\omega(t)$ is a linear function in the first order approximation of the perturbation. The slow motion of the line of apsides is usually called *precession*.

For example, Figure 4 shows the evolution of the parameter ω for an orbit compared with the parameter of the same orbit without oblateness. The elements used are $e = 0.64$ and $a = 0.6098$.

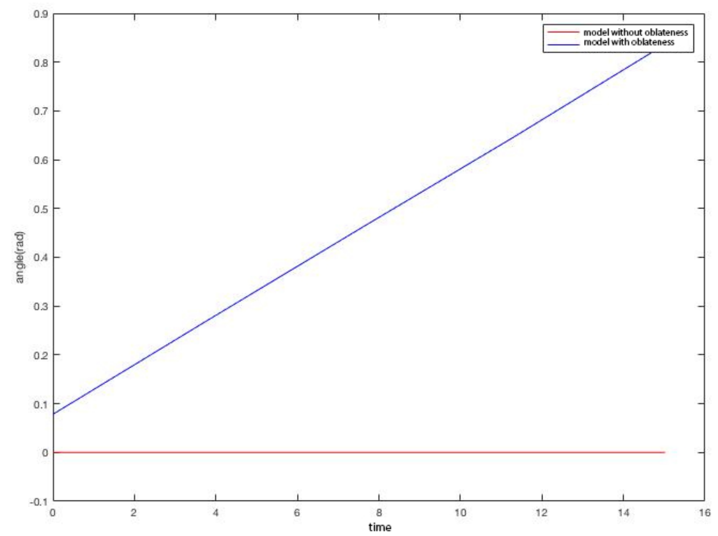

Figure 4: Angle of periapsis

Now, let's see how $\omega(t)$ depends on the eccentricity and the semi-major axis of an orbit. First, with a constant semi-major axis $a = 1$ and varying the eccentricity, we can see how the precessing speed increases with the eccentricity.

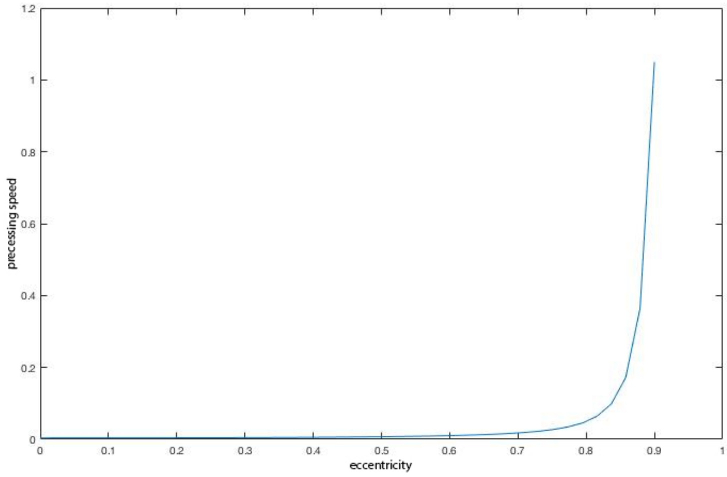

Figure 5: Eccentricity variation speed

On the other hand, with a fixed eccentricity $e = 0.3$, as the semi-major axis increases, the precessing speed decreases, as shown on the next figure.

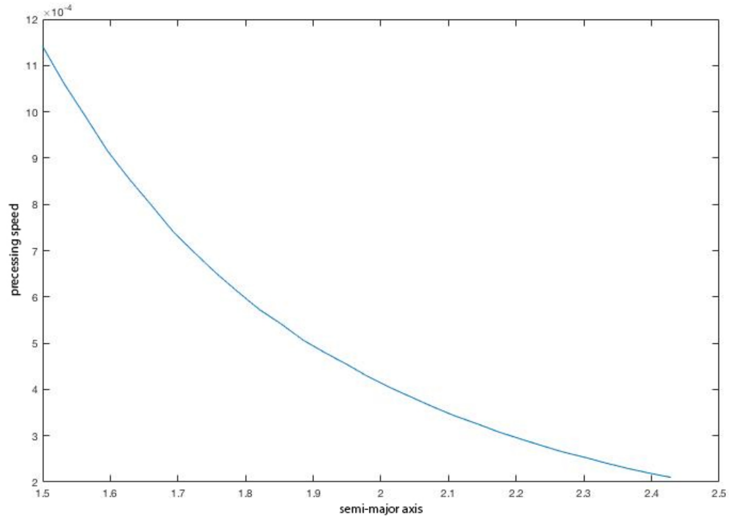

Figure 6: Semi-major axis variation speed

These pertorbations are explained in [7].

4 Periodic and almost-periodic solutions

4.1 Definition of periodic orbits and almost periodic orbits

Let's consider the following autonomous differential equations system

$$\dot{x} = f(x)$$

with f satisfying existence and uniqueness of solutions conditions.
Then, we define the solution that at time t_0 passes through x_0 as $\phi(t) = \phi(t; t_0, x_0)$.

A solution $\phi(t)$ is periodic of period T if $\phi(t) = \phi(t+T)$, $\forall t \in I$, where I is the maxium region of time for the solution.

Another important definition is the one of almost periodic solutions. A solution $\phi(t)$ is almost periodic if, $\forall \epsilon > 0$, any interval of length $l(\epsilon)$ contains a number T so that

$$\|\phi(t+T) - \phi(t)\| < \epsilon, \quad \forall t \in I$$

Let's see an example to understand what is an almost periodic solution. Working on the torus $\mathbb{T} = [0,1] \times [0,1]/_{\sim}$, where

$$(x_1, x_2) \sim (y_1, y_2) \Leftrightarrow \begin{cases} x_1 = y_1, x_2 = 0, y_2 = 1 \\ \text{or} \\ x_2 = y_2, x_1 = 0, y_1 = 1 \end{cases},$$

suppose that we have the following differential equation:

$$\dot{\mathbf{x}} = \mathbf{v}$$

where $\mathbf{v}$ is a constant vector. The solution is obvious:

$$\mathbf{x}(t) = \mathbf{x}_0 + t\mathbf{v}$$

If $\mathbf{v} = (v_1, v_2)$, the slope of this line will be $m = \frac{v_2}{v_1}$. If $m \in \mathbb{Q}$, the solution is periodic: some laps later, the solution will meet its initial condition, and because of the uniqueness of the solution, it will be periodic. On the other hand if $m \notin \mathbb{Q}$, the solution is almost-periodic: the orbits make a dense set that ends up filling densely the whole box, but the solution will never meet the initial condition again. This result was proven by Jacobi in 1845, see [2] for details. Figure 7 show different examples, all of them with initial conditions $\dot{x}_0 = (0.1, 0.1)$ and different slopes and laps number.

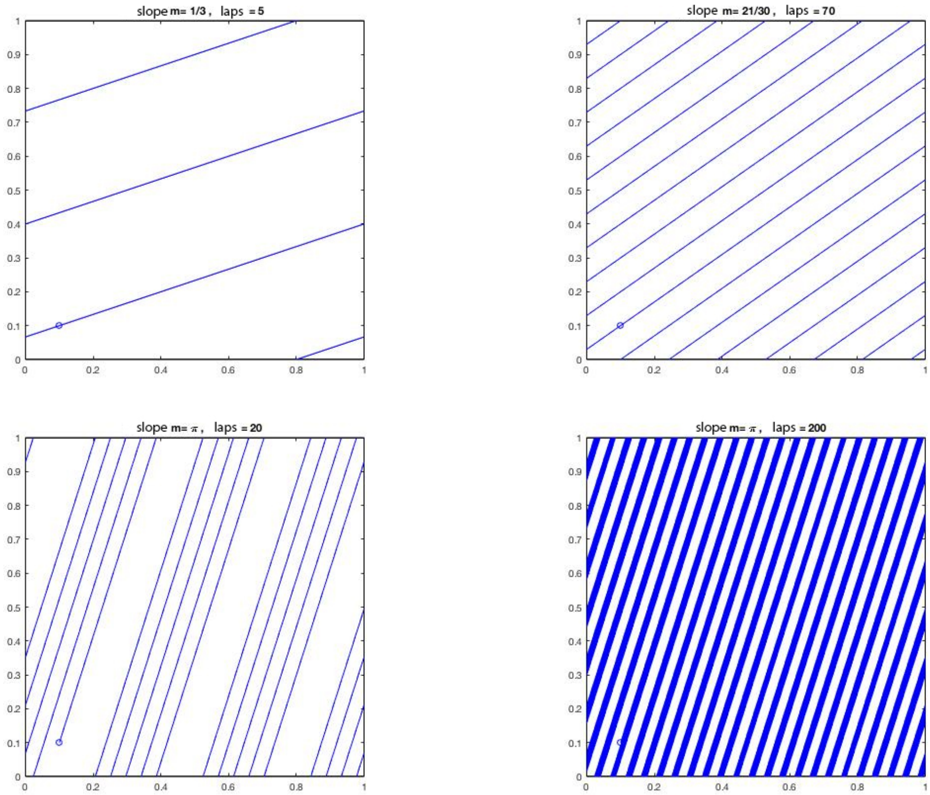

Figure 7: Periodic and almost-periodic solutions on a torus

4.2 Symmetries of the equations

Let's see some important results that will end up in a theorem that will allow us to find periodic or almost periodic solutions for our system.
We consider the following vector, which contains the positions of both bodies
$\gamma(t) = [x_1(t), y_1(t), x_2(t), y_2(t)]$ and the vector of velocities $\dot{\gamma}(t) = [\dot{x}_1(t), \dot{y}_1(t), \dot{x}_2(t), \dot{y}_2(t)]$, so the solution vector is $\phi(t) = (\gamma(t), \dot{\gamma}(t))$.

The differential equation is

$$\frac{d}{dt}(\gamma, \dot{\gamma}) = F(\gamma, \dot{\gamma}) \tag{1}$$

We will write the function of the differential equation as $F(\gamma, \dot{\gamma}) = (F_1(\dot{\gamma}), F_2(\gamma))$, where

$$F_1(\dot{\gamma})^\top = \begin{pmatrix} \dot{x}_1(t) \\ \dot{y}_1(t) \\ \dot{x}_2(t) \\ \dot{y}_2(t) \end{pmatrix} \quad F_2(\gamma)^\top = \begin{pmatrix} -\frac{x_1}{r_1^3} - \frac{3}{2}\frac{{R_S^*}^2 J_2 x_1}{r_1^5} - m_2\frac{x_1 - x_2}{r^3} \\ -\frac{y_1}{r_1^3} - \frac{3}{2}\frac{{R_S^*}^2 J_2 y_1}{r_1^5} - m_2\frac{y_1 - y_2}{r^3} \\ -\frac{x_2}{r_2^3} - \frac{3}{2}\frac{{R_S^*}^2 J_2 x_2}{r_2^5} - m_1\frac{x_2 - x_1}{r^3} \\ -\frac{y_2}{r_2^3} - \frac{3}{2}\frac{{R_S^*}^2 J_2 y_2}{r_2^5} - m_1\frac{y_2 - y_1}{r^3} \end{pmatrix}$$

where $r = \sqrt{(x_2 - x_1)^2 + (y_2 - y_1)^2}$, $r_i = \sqrt{x_i^2 + y_i^2}$ and $M^\top$ means the transpose of the matrix M.

We will prove a fundamental result on the symmetry of the equations which will be used to show the existence of periodic or quasi-periodic solutions of the system.

Lemma 1: Symmetry invariance. Let S be the Symmetry

$$S(x_1, y_1, x_2, y_2, \dot{x}_1, \dot{y}_1, \dot{x}_2, \dot{y}_2) = (x_1, -y_1, x_2, -y_2, \dot{x}_1, -\dot{y}_1, \dot{x}_2, -\dot{y}_2).$$

If $(\gamma(t), \dot{\gamma}(t))$ is a solution of (1) with initial conditions $(\gamma(0), \dot{\gamma}(0))$ defined in $t \in [0, T]$ then $S[\gamma(t), \dot{\gamma}(t)]$ is a solution of (1) with initial values $S(\gamma(0), \dot{\gamma}(0))$ defined for all $t \in [0, T]$.

Proof: It is obvious that the solution passes through $S(\gamma(0), \dot{\gamma}(0))$ by definition. Let's see that $S(\gamma(t), \dot{\gamma}(t))$ is a solution of the differential equation. What we want to see is that if $\frac{d}{dt}(\gamma, \dot{\gamma}) = F((\gamma, \dot{\gamma}))$, then $\frac{d}{dt}S(\gamma, \dot{\gamma}) = F(S(\gamma, \dot{\gamma}))$.

Let's see it for F_1:

$$\frac{d}{dt}S(\gamma) = \frac{d}{dt}(x_1, -y_1, x_2, -y_2) = (\dot{x}_1, -\dot{y}_1, \dot{x}_2, -\dot{y}_2) = \\ = S(\dot{x}_1, \dot{y}_1, \dot{x}_2, \dot{y}_2) = F_1(S(\dot{\gamma}))$$

Let's see it now for F_2: First, we notice that both r and r_i are invariant under S. Now, checking it for the derivatives of the components $\dot{x}_1$ and $\dot{y}_1$ (checking this for the second body is analogous) we obtain:

$$\frac{d}{dt}(\dot{x_1}) = -\frac{x_1}{r_1^3} - \frac{3}{2}\frac{{R_S^*}^2 J_2 x_1}{r_1^5} - m_2\frac{x_1 - x_2}{r^3}$$

$$\begin{aligned} \frac{d}{dt}(-\dot{y}_1) &= -\left(-\frac{y_1}{r_1^3} - \frac{3}{2}\frac{{R_S^*}^2 J_2 y_1}{r_1^5} - m_2\frac{y_1 - y_2}{r^3}\right) \\ &= -\frac{(-y_1)}{r_1^3} - \frac{3}{2}\frac{{R_S^*}^2 J_2(-y_1)}{r_1^5} - m_2\frac{(-y_1) - (-y_2)}{r^3} \end{aligned}$$

Doing the same for the second body, we obtain that the derivatives are evaluated on the simetric points by S, that means:

$$\frac{d}{dt}S(\dot{\gamma}) = F_2(S(\gamma))$$

Thus, $S(\gamma, \dot{\gamma})$ satisfies the differential equation and that means that it is a solution too, defined in $[0, T]$. □

Lemma 2: Reversing the trajectory. If $(\gamma(t), \dot{\gamma}(t))$ is a solution of (1) with initial values $(\gamma(0), \dot{\gamma}(0))$ defined in $t \in [0, T]$, then $(\gamma(-t), -\dot{\gamma}(-t))$ is a solution of (1) with initial values $(\gamma(T), -\dot{\gamma}(T))$ defined in $t \in [-T, 0]$.

Proof:
If we evaluate the new solution in $-T$ we automatically get the initial condition. Let's see now that the function is a solution of the differential equation.

Defining $psi(t) = \gamma(-t)$, we see that:

$$\frac{d\psi(t)}{dt} = -\frac{d\gamma(-t)}{dt} = -F_1(\gamma(-t)) = -F_1(\psi(t))$$

As $F_1(\gamma(t)) = \dot{\gamma}(t)$, then $\frac{d\psi(t)}{dt} = -\dot{\psi}(t) = -\dot{\gamma}(-t)$.
Let's see the derivative of the component $-\dot{\psi}(t)$:

$$\frac{d}{dt}(-\dot{\psi}(t)) = \frac{d}{dt}\gamma(-t) = F_2(\gamma(-t)) = F_2(\psi(t))$$

Thus, $\psi(t)$ is a solution of the equation and it is defined in $[-T, 0]$. □

Lemma 3: Rotation invariance. If R is a rotation of angle α in $\mathbb{R}^2$, we consider

$R(\gamma(t), \dot\gamma(t)) = (R(x_1, y_1), R(x_2, y_2), R(\dot x_1, \dot y_1), R(\dot x_2, \dot y_2))$. If $(\gamma(t), \dot\gamma(t))$ is a solution of (1) with initial values $(\gamma(0), \dot\gamma(0))$ defined in $t \in [0, T]$, then $R(\gamma(t), \dot\gamma(t))$ is a solution of (1) with initial values $R(\gamma(0), \dot\gamma(0))$ defined in $t \in [0, T]$.

Proof: Let M be the matrix of the rotation of angle α in $\mathbb{R}^2$, so that

$$R(x, y) = M \cdot (x, y)^\top$$

As before, it is obvious that the initial condition is met. We only need to see the equations for each component. For γ:

$$\frac{d}{dt}R((x_1, y_1)) = \frac{d}{dt}(M(x_1, y_1)) = M(\dot x_1, \dot y_1)$$

We get the same for the second body and, thus, $\frac{d}{dt}R(\gamma) = F_1(R(\dot\gamma))$.

Let's see now what happens with the derivative of $R(\gamma(t))$. To simplify notation, we will write $S = \sin(\alpha)$ and $C = \cos(\alpha)$.

$$\begin{aligned}
\frac{d}{dt}R(\dot x_1) &= \frac{d}{dt}(C\dot x_1 - S\dot y_1) \\
&= C\left(-\frac{x_1}{r_1^3} - \frac{3}{2}\frac{{R_S^*}^2 J_2 x_1}{r_1^5} - m_2\frac{x_1 - x_2}{r^3}\right) - S\left(-\frac{y_1}{r_1^3} - \frac{3}{2}\frac{{R_S^*}^2 J_2 y_2}{r_1^5} - m_2\frac{y_1 - y_2}{r^3}\right) \\
&= -\frac{(Cx_1 - Sy_1)}{r_1^3} - \frac{3}{2}\frac{{R_S^*}^2 J_2 (Cx_1 - Sy_1)}{r_1^5} - m_2\frac{(Cx_1 - Sy_1) - (Cx_2 - Sy_2)}{r^3} \\
&= -\frac{R(x_1)}{r_1^3} - \frac{3}{2}\frac{{R_S^*}^2 J_2 R(x_1)}{r_1^5} - m_2\frac{R(x_1) - R(x_2)}{r^3}
\end{aligned}$$

$$\begin{aligned}
\frac{d}{dt}R(\dot y_1) &= \frac{d}{dt}(S\dot x_1 + C\dot y_1) \\
&= S\left(-\frac{x_1}{r_1^3} - \frac{3}{2}\frac{{R_S^*}^2 J_2 x_1}{r_1^5} - m_2\frac{x_1 - x_2}{r^3}\right) + C\left(-\frac{y_1}{r_1^3} - \frac{3}{2}\frac{{R_S^*}^2 J_2 y_1}{r_1^5} - m_2\frac{y_1 - y_2}{r^3}\right) \\
&= -\frac{Sx_1 + Cy_1}{r_1^3} - \frac{3}{2}\frac{{R_S^*}^2 J_2 (Sx_1 + Cy_1)}{r_1^5} - m_2\frac{(Sx_1 + Cy_1) - (Sx_2 + Cy_2)}{r^3} \\
&= -\frac{R(y_1)}{r_1^3} - \frac{3}{2}\frac{{R_S^*}^2 J_2 R(y_1)}{r_1^5} - m_2\frac{R(y_1) - R(y_2)}{r^3}
\end{aligned}$$

The same is obtained for the second body and thus, $\frac{d}{dt}(R(\dot\gamma)) = F_2(R(\gamma))$. $\square$

Lemma 4: Let $(\gamma(t), \dot\gamma(t))$, $t \in [0, T]$ be a solution with $y_1(0) = y_2(0) = 0$ and $\dot x_1(0) = \dot x_2(0) = 0$. Let $(\bar\gamma(t), \dot{\bar\gamma}(t))$ be the simetric solution travelled in the reverse way, obtanied from (1) and (2). Then we can join both solutions and define

$$\tilde\gamma(t) = \begin{cases} \bar\gamma(t) \text{ if } t \in [-T, 0] \\ \gamma(t) \text{ if } t \in [0, T] \end{cases}$$

Proof:
By construction, we have that $\tilde\gamma(t)$ meets the differential equations. We only need to see that both parts join continously and with continous derivative.

For the positions:
Evaluating in $t = 0$ both parts, we get that $\bar\gamma(0) = (x_1(0), 0, x_2(0), 0) = \gamma(0)$.
For the velocities:

Evaluating in $t = 0$ both parts, we get that $\dot{\bar{\gamma}}(0) = (0, \dot{y}_1(0), 0, \dot{y}_2(0))$ and
$\dot{\gamma}(0) = (0, \dot{y}_1(0), 0, \dot{y}_2(0))$.

Thus we have just seen that they coincide. □

Theorem: Suppose there exist two lines $A_0 x + B_0 y = 0$ and $Ax + By = 0$ and a solution $\gamma(t)$ such that

$$A_0 x_i(0) + B_0 y_i(0) = 0, A_0 \dot{y}_i(0) - B_0 \dot{x}_i(0) = 0 \quad i = 1, 2$$

and

$$A x_i(T) + B y_i(T) = 0, A \dot{y}_i(T) - B \dot{x}_i(T) = 0 \quad i = 1, 2$$

for some $T \geq 0$. Intuitively, the solution starts over a line with a perpendicular velocity to it, and after a time T it is again over a line with perpendicular velocities to this line.

Then this solution can be extended to a periodic or quasi-periodic (periodic in a rotating frame) solution of the system.

Proof: Due to the invariance under rotation we can take $A_0 = 0$ so that at $t = 0$ the bodies are on the x-axis with $\dot{x}_1(0) = 0$ and $\dot{x}_2(0) = 0$. Let $Ax - By = 0$ be the line symmetric to $Ax + By = 0$ with respect to the x-axis and α the angle between those lines. According to Lemma 4, there exist a solution $\overline{\gamma}(t)$ $t \in [0, 2T]$, such that

$$A x_i(0) + B y_i(0) = 0, A \dot{y}_i(0) - B \dot{x}_i(0) = 0 \qquad i = 1, 2$$

$$y_i(T) = 0, \dot{x}_i(T) = 0 \qquad i = 1, 2$$

$$A x_i(2T) + B y_i(2T) = 0, A \dot{y}_i(2T) - B \dot{x}_i(2T) = 0 \qquad i = 1, 2$$

and

$$\dot{y}_i(0) = \dot{y}_i(2T), \dot{x}_i(0) = -\dot{x}_i(2T) \qquad i = 1, 2.$$

This means $S(\gamma(0), \dot{\gamma}(0)) = (\gamma(2T), \dot{\gamma}(2T))$, where S is the rotation of angle α. Any trajectory obtained by rotating $\gamma(t)$ is a solution. Then we can join any number of arcs and this will be a solution of the system. This solution will be periodic if $\alpha = \frac{p}{q}\pi$ and almost-periodic otherwise, see [2] for details.

4.3 Using the symmetries

To use the theorem we need to find solutions where the bodies are all alligned on a line, with velocities perpendicular to that line on two different moments, with two lines not necessarily being the same.

As the masses of the coorbital satellites are very small we can we can consider their motion as elliptic except when the bodies are close to each other.

This is when the first difficulty of using an elliptic model comes compared with a circular model: there are only two moments when a body has a velocity which is perpendicular to a line passing throught the origin, that is, when its radial velocity $\dot{r} = 0$. That happens in the periapsis or in the apoapsis, while in a circular orbit, the condition $\dot{r} = 0$ is always satisfied.

While in the circular case, if the bodies start over a line with $\dot{r}_i(0) = 0$, we know that after a certain T multiple of the periods of both bodies, the solution will be again on the initial conditions, obviously with $\dot{r}_i(T) = 0$, ie this is a periodic solution.

On the elliptic case, those moments when $\dot{r} = 0$ are harder to find, and not only that, as the periapsis and apoapsis of both bodies are moving, as a consequence of oblateness.

With that in mind what we need to find is a moment when the bodies are again aligned in a different line, with perpendicular velocities. Then, applying the theorem seen in section 4.2, the solution will be at least almost-periodic, or periodic in the best case.

Checking whether a solution is periodic or almost-periodic is very difficult if we are working in a finite precission machine, as we need to know whether the difference of angles between the first and second line is a rational or irrational multiple of π. With finite precission, we will never be able to check if that difference is an irrational number, so we will have to conform with knowing that the solutions are at least almost-periodic.

Two different cases will be studied:

- Restricted case with $\mu_1 = 0$
- Full problem with $\mu_1 \neq 0$

In the first case, the movement of the second body is periodic in an inertial frame with period T_0,and the function of its radius too. Because of that, $\dot{r}_2(T) = 0$ for $T = nT_0$, and this does not depend on the movement of the first body.

5 Numerical Analysis of the system

As stated in section 2.4, we need to find initial conditions so that the bodies can be found after a certain time over a line with velocities being perpendicular to this line.

Let's recall our system. We will start our simulations with the two bodies over the X-axis with a velocity being perpendicular to this axis, so we will have only 2 initial conditions for each body. The parameters for each body are shown in this table.

	Body 1	Body 2
Mass	μ_1	μ_2
Initial Position	x_1^0	x_2^0
Initial Speed	$\dot{y}_1^0$	$\dot{y}_2^0$

We should remark that $y_1^0 = y_2^0 = \dot{x}_1^0 = \dot{x}_2^0 = 0$, and they are fixed so we don't need to look at them.

We will carry out two groups of simulations: on the first one, we will consider the restricted problem
($\mu_1 = 0$) and on the second one, the full problem ($\mu_1 \neq 0$). In both cases, the initial conditions of the second body x_2^0 and $\dot{y}_2^0$ are fixed, and we will use as variables the initial conditions of the first body.

We will use equations that determine when both bodies have perpendicular velocities to the same line, and we will solve them numerically with fsolve. It is important to note that the equations are different for the restricted problem and the full problem. The differential equations are integrated using a Runge-Kutta 7(8) with automatic adjustment of the stepsize with local truncation error $\leq 10^{-12}$ (see apendix A).

5.1 Periodic orbits of the restricted problem

It is easier to find periodic or almost-periodic solutions for the restricted problem ($\mu_1 = 0$). This is because in this case, the second body dynamics are not affected by the first body, so independently of the first body initial conditions, the orbit of the second body will always be the same (it only depends from its initial conditions).

If the period of the second body is T_0, we need to look at a time $T = nT_0$ where $\dot{r}_2(T) = 0$, and we need to find initial conditions for the first body so that, at time T:

- $\dot{r}_1(T) = 0$ (velocity of the body is perpendicular to the line that unites the origin and the body)
- $\theta_1(T) = \theta_2(T)$ (both bodys and the origin are all aligned)

The equations that we need to solve are:

$$\begin{cases} \dot{r}_1(T, x_1^0, \dot{y}_1^0) = 0 \\ \theta_1(T, x_1^0, \dot{y}_1^0) = \theta_2(T) + \pi \end{cases}$$

It is important to note that the value $\theta_2(T)$ is fixed and doesn't depend on the initial conditions that we are looking for.

Let's check a case where our solver algorithm converges to a solution. After a first exploration, these parameters seem to have a solution relatively close to them.

$$\begin{array}{ll} \mu_1 = 0 & \mu_2 = 1 \times 10^{-4} \\ x_1^0 = 1 & x_2^0 = -1.00033 \\ \dot{y}_1^0 = 1.0038 & \dot{y}_2^0 = -1.00883504082627 \end{array}$$

At time $T = 334.5426539$, those parameters and initial conditions return the following solution.

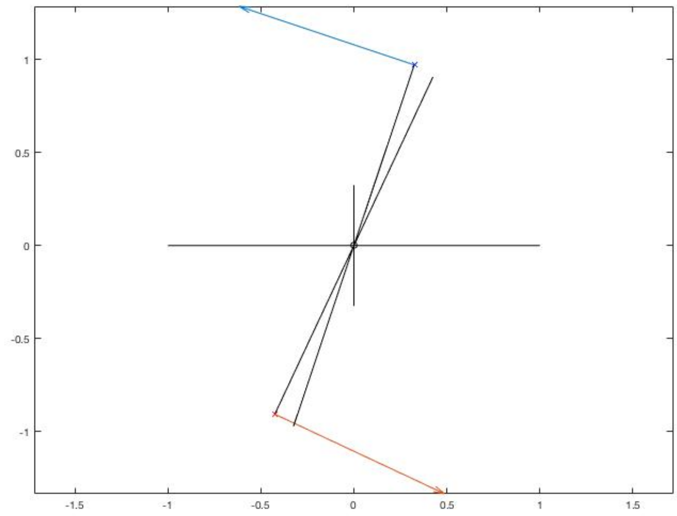

Figure 8: Solution at time T. Both bodies have $\dot{r} = 0$, but they are not alligned with the origin.

We expect this point to have a good behavior with the algorithm because both bodies have already $\dot{r}_i = 0$, the only thing that we have to adjust is the difference between the lines they are lying on.

Our solver returns the new initial conditions $x_1^0 = 0.9927674$ and $\dot{y}_1^0 = 1.0106799$, we can plot the system at the chosen time T:

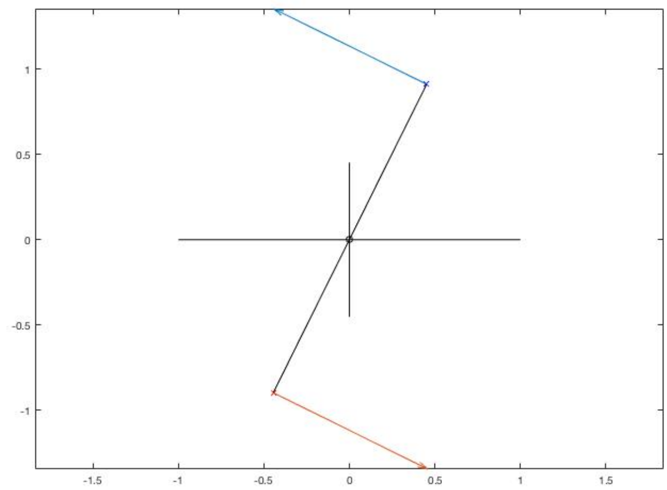

Figure 9: Solution at time T with both bodies aligned and with $\dot{r} = 0$

We can visually check that both bodies lie on the same line, and their velocities are now perpendicular to that line so this is at least an almost-periodic solution.
A plot of the solution in a rotating frame is shown in the figure 10.

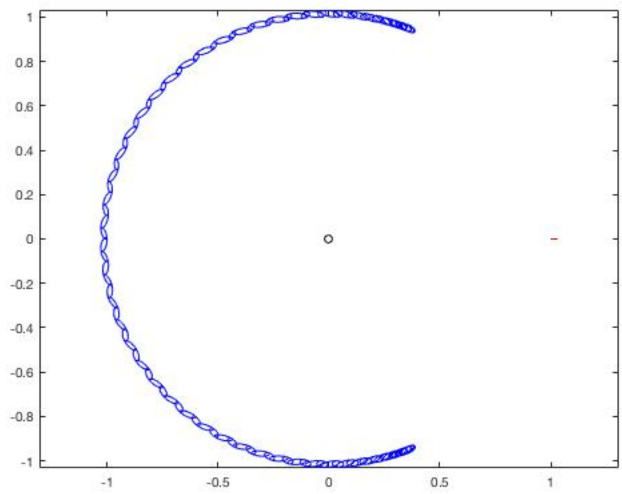

Figure 10: Horseshoe orbit

Varying the parameter μ_2 and applying our algorithm, we can find a family of initial conditions for periodic solutions for each value of μ_2. These are shown in the following table.

μ_2	x_1^0	$\dot{y}_1^0$
1×10^{-5}	0.999427160999146	1.00322694684416
1.2×10^{-4}	0.999988788595394	1.00378879733339
2.3×10^{-4}	1.00178440924134	1.00558020314097
3.4×10^{-4}	1.00272321897236	1.00651091214703
4.5×10^{-4}	1.00275453562599	1.00649912457105
5.6×10^{-4}	1.00782017544763	1.01131828365252
6.7×10^{-4}	0.998437829724124	1.00218180597688
7.8×10^{-4}	0.999276841537461	1.00306833523972
8.9×10^{-4}	1.00047682064924	1.00427712045779
1×10^{-3}	1.00279055823845	1.00660329668551

Their rotating frames are shown in figure 11, sorted from left to right and top to bottom.

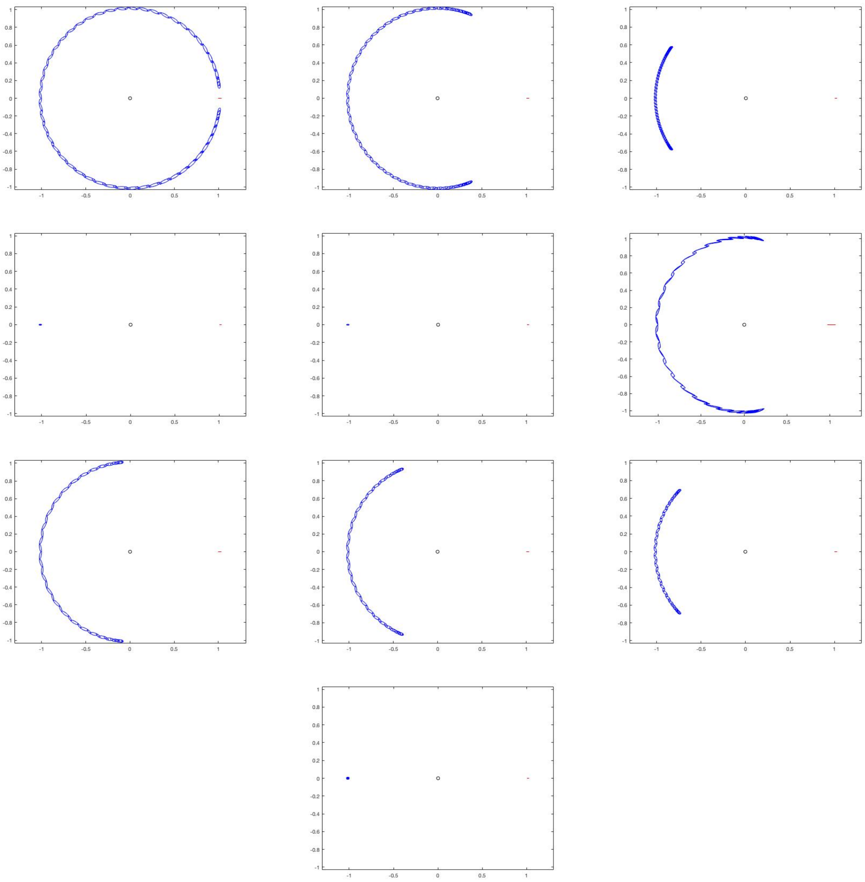

Figure 11: Rotating frames

The minimum angle difference between both bodies of each figure is

μ_2	angle
1×10^{-5}	1.108076095925321
1.2×10^{-4}	1.17614801156617
2.3×10^{-4}	2.52554434625066
3.4×10^{-4}	3.13593391588195
4.5×10^{-4}	3.13624829108378
5.6×10^{-4}	1.33463092538931
6.7×10^{-4}	1.64507897870288
7.8×10^{-4}	1.96181115978572
8.9×10^{-4}	2.37710980150335
1×10^{-3}	3.1297852045954

Looking at the table of the initial conditions and the rotating frames, and seeing the sudden differences of the initial conditions, we can guess that we have found three different families of solutions to the problem.

5.2 Periodic orbits of the full problem

For the general three body problem ($\mu_1 \neq 0$), the system becomes more complicated, because changing the initial conditions for the first body also changes the orbit for the second body. That means that the fixed time T where $\dot{r}_2 = 0$ will not be constant this time, so we add a third equation to our system, and we use T as an unknown leaving us with the following system, with x_2^0 and $\dot{y}_2^0$ fixed as before:

$$\begin{cases} \dot{r}_1(T, x_1^0, \dot{y}_1^0) = 0 \\ \dot{r}_2(T, x_1^0, \dot{y}_1^0) = 0 \\ \theta_1(T, x_1^0, \dot{y}_1^0) = \theta_2(T, x_1^0, \dot{y}_1^0) + \pi \end{cases}$$

Again, a case where we can check convergence of the solver is the following:

$$\begin{array}{ll} \mu_1 = 9.2908 \times 10^{-8} & \mu_2 = 3.3477 \times 10^{-7} \\ x_1^0 = 1 & x_2^0 = -1.00033 \\ \dot{y}_1^0 = 1.0034 & \dot{y}_2^0 = -1.00473504082627 \end{array}$$

Figure 12 shows both bodies and their velocities at time $T = 1349.22841802281$, drawing a line that connects each body and the origin.

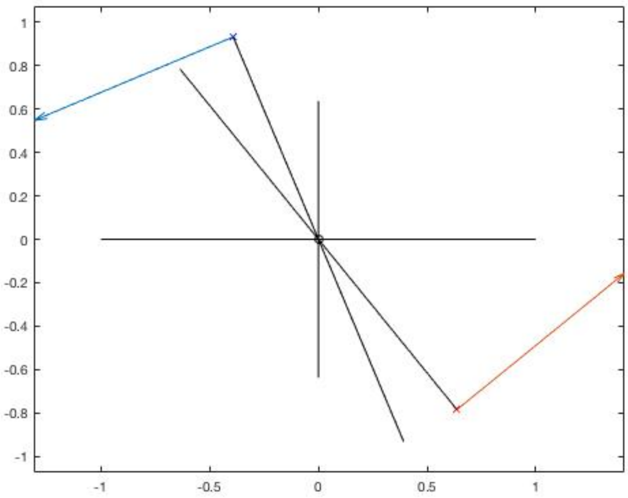

Figure 12: Solution at time T. Both bodies have almost $\dot{r} = 0$ and they are almost aligned.

Again, this point and time seems to be a good one to find our almost-periodic or periodic solution. Applying our solver returns us the following values:

$$T = 1349.22841802281 \quad x_1^0 = 1.00003386261033 \quad \dot{y}_1^0 = 1.00343383701262$$

At time T, our solution is again as we expected to be.

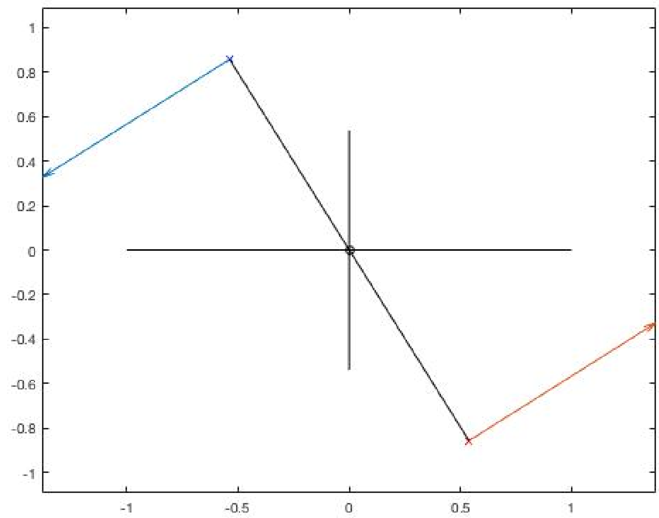

Figure 13: Solution at time T. Both bodies have $\dot{r} = 0$ and are aligned.

This periodic or almost-periodic solution describes a horseshoe orbit in a rotating frame as shown in figure 14.

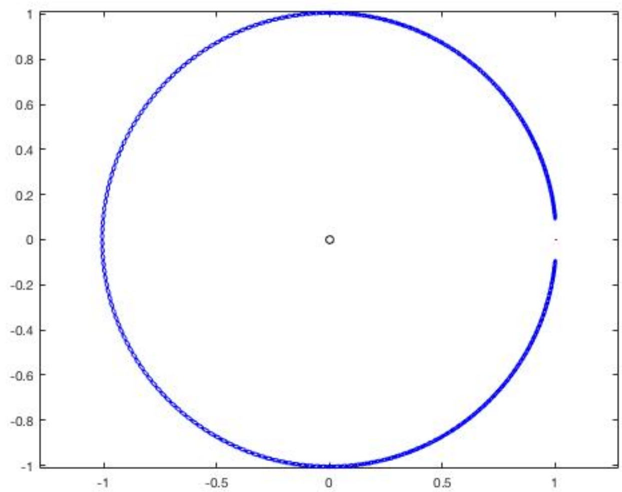

Figure 14: Horseshoe orbit travelled until the conditions of perpendicularity and alignment are met.

In addition, we can try to find a family of solutions for different masses, as we did with the restricted case. For example, increasing the value of μ_2 we find the following table:

μ_2	T	x_1^0	$\dot{y}_1^0$
3.3477×10^{-7}	1349.22841802281	1.00003386261033	1.00343383701262
4.3477×10^{-7}	1349.34655894602	1.00449173806666	0.998977353941602
1.53477×10^{-6}	1350.2279594649	0.999919252266667	1.00352618893254
2.63477×10^{-6}	1350.2395210253	1.00068303183094	1.00278827875082
3.73477×10^{-6}	1350.34150501394	1.00131550582251	1.00220225335778
4.83477×10^{-6}	1350.38103086364	1.0005313201026	1.00304586495594
5.93477×10^{-6}	1350.40702207895	1.00210391613525	1.00154616812146
7.03477×10^{-6}	1350.42582849255	1.00049280066645	1.00323747756741
8.13477×10^{-6}	1350.440172592	1.00059763933597	1.00322563315522
9.23477×10^{-6}	1350.44831124301	1.00493195095702	0.999008974169544
1.033477×10^{-5}	1350.46143837533	1.00097278974736	1.00307704535998

Their respective horseshoe orbits are shown in figure 15, sorted from left to right and top to bottom.

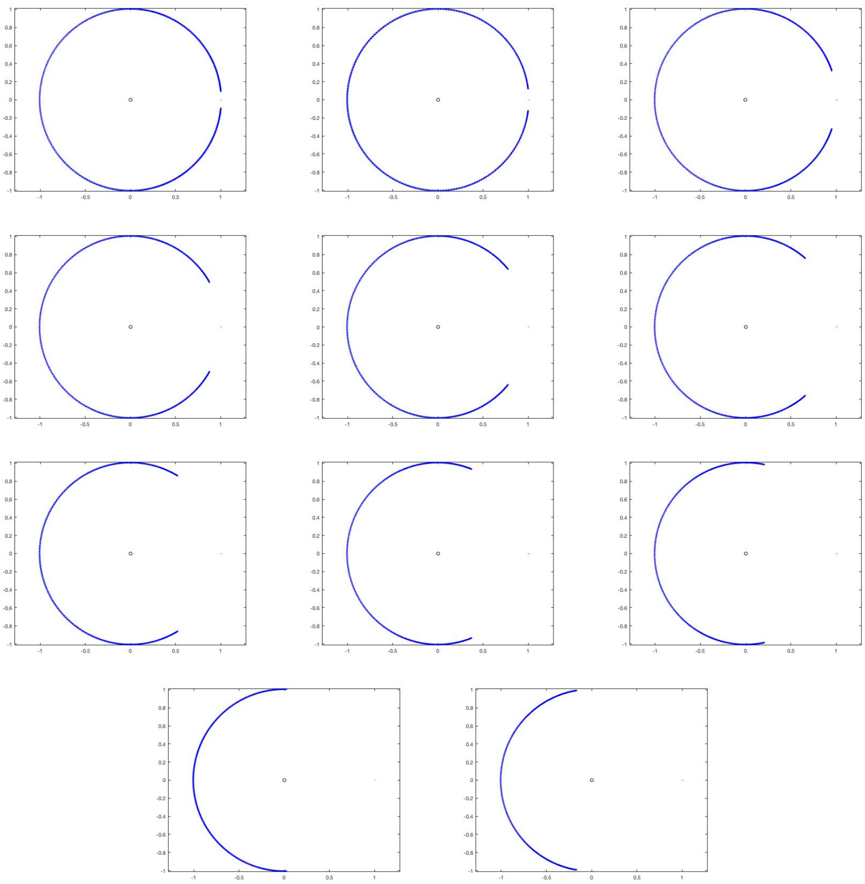

Figure 15: Rotating frames

The minimum angle difference between both bodies of each figure is

μ_2	angle
3.3477×10^{-7}	0.0867734154083654
4.3477×10^{-7}	0.116206166469321
1.53477×10^{-6}	0.319778712279022
2.63477×10^{-6}	0.507390869815747
3.73477×10^{-6}	0.682789847759622
4.83477×10^{-6}	0.850163839669154
5.93477×10^{-6}	1.01928657172119
7.03477×10^{-6}	1.18537325956951
8.13477×10^{-6}	1.3582054103236
9.23477×10^{-6}	1.54057528107651
1.033477×10^{-5}	1.73247749471697

If we continue increasing μ_2, the algorithm stops converging beyond 1.033477×10^{-5}, so the family of solutions cannot be followed any further.

6 Conclusions and future work

The algorithms and the model have worked pretty well. The solution orbits were smooth and close to the real ones, showing the orbit-swap phenomen.

More important, we have found periodic or almost-periodic solutions, both for the restricted problem and the full problem. More than that, given a periodic or almost-periodic solution we have seen that there exists a family of periodic or almost-periodic solutions around it, varying the mass parameters of a body, and it seems that finding these families is not difficult.

Future work that could be done to expand what we have found is:

- Ways of looking for periodic orbits and families sistematically or anallitically.
- Methods to distinguish between periodic and almost-periodic solutions.
- An analysis of convergence regions of initial conditions to study patterns in the distribution of initial conditions that return a periodic or almost-periodic solution.
- Working in three dimensions and compare results.

7 Apendix A: The Runge-Kutta 7(8) method

The method that we use in our simulations is an embedded Runge-Lutta of orders 7 and 8. The Butcher tableau of this method is on the next page.

The reason of why we are using this method is for his great order, despite not having such a big computational cost.

A Runge-Kutta only needs to evaluate the differential equation function multiple times, which isn't a ver intensive task. For our simulations we need high accuracy, as we are checking very sensible things, such as perpendicular angles, and not enough accuracy could give us false results. For this reason, a non-embedded Runge-Kutta or an embeded Runge-Kutta of orders 4 and 5 is not enough.

As the method is embedded, it adjusts the stepsize automatically, comparing the solutions of order 7 and 8, and that gives us high control on the accuracy of the solutions, allowing us to even demand a certain number of significant figures.

$$
A = \begin{pmatrix}
0 & 0 & 0 & 0 & 0 & 0 & 0 & 0 & 0 & 0 & 0 & 0 & 0 \\
\frac{1}{18} & 0 & 0 & 0 & 0 & 0 & 0 & 0 & 0 & 0 & 0 & 0 & 0 \\
\frac{1}{48} & \frac{1}{16} & 0 & 0 & 0 & 0 & 0 & 0 & 0 & 0 & 0 & 0 & 0 \\
\frac{1}{32} & 0 & \frac{3}{32} & 0 & 0 & 0 & 0 & 0 & 0 & 0 & 0 & 0 & 0 \\
\frac{5}{16} & 0 & \frac{-75}{64} & \frac{75}{64} & 0 & 0 & 0 & 0 & 0 & 0 & 0 & 0 & 0 \\
\frac{3}{80} & 0 & 0 & \frac{3}{16} & \frac{3}{20} & 0 & 0 & 0 & 0 & 0 & 0 & 0 & 0 \\
\frac{29443841}{614563906} & 0 & 0 & \frac{77736538}{692538347} & \frac{-28693883}{1125000000} & \frac{23124283}{1800000000} & 0 & 0 & 0 & 0 & 0 & 0 & 0 \\
\frac{16016141}{946692911} & 0 & 0 & \frac{61564180}{158732637} & \frac{22789713}{633445777} & \frac{545815736}{2771057229} & \frac{-180193667}{1043307555} & 0 & 0 & 0 & 0 & 0 & 0 \\
\frac{39632708}{573591083} & 0 & 0 & \frac{-433636366}{683701615} & \frac{-421739975}{2616292301} & \frac{100302831}{723423059} & \frac{790204164}{839813087} & \frac{800635310}{3783071287} & 0 & 0 & 0 & 0 & 0 \\
\frac{246121993}{1340847787} & 0 & 0 & \frac{-37695042795}{15268766246} & \frac{-309121744}{1061227803} & \frac{-12992083}{490766935} & \frac{6005943493}{2108947869} & \frac{393006217}{1396673457} & \frac{123872331}{1001029789} & 0 & 0 & 0 & 0 \\
\frac{-1028468189}{846180014} & 0 & 0 & \frac{8478235783}{508512852} & \frac{1311729495}{1432422823} & \frac{-10304129995}{1701304382} & \frac{-48777925059}{3047939560} & \frac{15336726248}{1032824649} & \frac{-45442868181}{3398467696} & \frac{3065993473}{597172653} & 0 & 0 & 0 \\
\frac{185892177}{718116043} & 0 & 0 & \frac{-3185094517}{667107341} & \frac{-477755414}{1098053517} & \frac{-703635378}{230739211} & \frac{5731566787}{1027545527} & \frac{5232866602}{850066563} & \frac{-4093664535}{808688257} & \frac{3962137247}{1805957418} & \frac{65686358}{487910083} & 0 & 0 \\
\frac{403863854}{491063109} & 0 & 0 & \frac{-5068492393}{434740067} & \frac{-411421997}{543043805} & \frac{652783627}{914296604} & \frac{11173962825}{925320556} & \frac{-13158990841}{6184727034} & \frac{3936647629}{1978049680} & \frac{-160528059}{685178525} & \frac{248638103}{1413531060} & 0 & 0
\end{pmatrix}
$$

$$
b = \begin{pmatrix} \frac{14005451}{335480064} & 0 & 0 & 0 & 0 & \frac{-59238493}{1068277825} & \frac{181606767}{758867731} & \frac{561292985}{797845732} & \frac{-1041891430}{1371343529} & \frac{760417239}{1151165299} & \frac{118820643}{751138087} & \frac{-528747749}{2220607170} & \frac{1}{4} \end{pmatrix}
$$

$$
b^* = \begin{pmatrix} \frac{13451932}{455176623} & 0 & 0 & 0 & 0 & \frac{-808719846}{976000145} & \frac{1757004468}{5645159321} & \frac{656045339}{265891186} & \frac{-3867574721}{1518517206} & \frac{465885868}{322736535} & \frac{53011238}{667516719} & \frac{2}{45} & 0 \end{pmatrix}
$$

$$
c = \begin{pmatrix} 0 & \frac{1}{18} & \frac{1}{12} & \frac{1}{8} & \frac{5}{16} & \frac{3}{8} & \frac{59}{400} & \frac{93}{200} & \frac{5490023248}{9719169821} & \frac{13}{20} & \frac{1201146811}{1299019798} & 1 & 1 \end{pmatrix}
$$

8 Bibliography

References

[1] J. D. Anderson and G. Schubert. Saturn's gravitational field, internal rotation, and interior structure. *Science*, 2007.

[2] V. I. Arnold and A. Avez. *Ergodic Problems of Classical Mechanics.* Addison Wesley, 1968.

[3] R. H. Battin. *An Introduction to the Mathematics and Methods of Astrodynamics.* Aiaa, 1999.

[4] J. D. Lambert. *Numerical Methods for Ordinary Differential Systems.* John Wiley & Sons, Inc., 1991.

[5] NASA. Jet propulsion laboratory. URL `https://jpl.nasa.gov`.

[6] M. Ollé and J. Llibre. Horseshoe periodic orbits for saturn coorbital satellites. *Celestial Mechanics and Dynamical Astronomy*, 2000.

[7] E. Stiefel and G. Scheifele. *Linear and Regular Celestial Mechanics.* Springer-Verlag Berlin Heidelberg, 1971.